ANALYSIS OF AIR TEMPERATURES IN THE CAVITY OF DOUBLE-SKIN FACADES

Dominika Husáriková[*,1], Erika Dolníková[1], Martin Lopušniak[1]

[*]dominika.husarikova@tuke.sk
[1]Institute of Architectural Engineering, Faculty of Civil Engineering, Technical University of Košice, Vysokoškolská 4, 042 00 Košice, Slovakia

Abstract

Non-optimal position of the blinds in double-skin facades can lead to overheating or heat loss. Spring temperature fluctuations and varying solar radiation provide ideal conditions for analysis, highlighting the impact of cavity geometry on thermal performance. This study examines the impact of blind positioning on the cavity air temperature in a double-skin facade during spring. Experimental measurements under different airflow modes showed that a smaller airflow circuit (mode A) produced greater temperature variations (0-7 K), whereas a larger circuit (mode D) resulted in smaller fluctuations (0-2 K).

Keywords

Double-skin facade, blinds, temperature, cavity

1 INTRODUCTION

Double-skin facades (DFSs) are a form of building cladding. They have gained popularity for their permeability, architectural design flexibility and energy savings [1]. DSFs consist of two layers of glazing separated by an air cavity, which can be naturally or mechanically ventilated to regulate heat transfer, reduce energy consumption, and enhance thermal comfort. The ability of DSFs to act as a thermal buffer zone between the indoor and outdoor environments makes them a crucial component in modern sustainable building design [2], [3]. DSFs have long been the subject of scientific research as an important element in reducing energy performance of buildings and improving the quality of the indoor environment. Architects and engineers are increasingly turning to advanced solutions like DSFs to meet sustainability goals as the demand for energy-efficient buildings rises in response to climate change [1], [4]. These facades contribute significantly to improving energy performance while reducing environmental impact. However, their design and implementation are complex, as they are influenced by a variety of factors, including climate conditions, facade configuration, cavity depth, ventilation mode, glazing properties, and operational strategies [5]. Each DSF application must be customized to the specific environmental and functional requirements of the building, making it impossible to apply a one-size-fits-all approach. Research in this area focuses primarily on achieving energy efficiency in the building and optimising the interaction between the indoor and outdoor environments. Design requires detailed knowledge and individual approach to each specific solution. An important aspect of the study of DSF is the influence of cavity geometry and configuration on its thermo-technical properties. Variations in cavity geometry, shading position or facade operation modes are variable factors that fundamentally affect the overall system performance [5], [6], [7]. Direct sunlight entering glazed facades can increase indoor temperatures, leading to higher cooling demands [8]. Research shows that double-skin facades without effective shading systems can lead to a 15–25% rise in cooling loads in warm climates due to excessive solar heat gain [9]. The positioning of blinds within the cavity plays a crucial role in controlling solar radiation, preventing overheating, and maintaining occupant comfort. Research has demonstrated that properly positioned blinds can reduce cooling loads, while adjustable blinds offer additional benefits in terms of optimizing daylighting and thermal comfort [8], [9]. Advanced DSFs integrate sensor-based control systems that adjust shading devices in real time based on daylight availability, indoor brightness levels, occupant preferences, and outdoor weather conditions [10]. A recent study conducted at Loughborough University introduced a specialized testing facility designed to assess the performance of ventilated double-skin facades under controlled conditions. The findings demonstrated that the thermal and airflow performance of double-skin facades is significantly influenced by key environmental factors, such as solar irradiance and outdoor air temperature. The presence of Venetian blinds within the ventilated cavity was found to divide the space into two distinct vertical

Received 07/02/2025/Accepted 07/05/2025/Published 30/09/2025 DOI 10.13164/juniorstav.2025.26102

chambers, altering temperature distribution and airflow characteristics. Notably, when the blinds were fully closed, the temperature in the front chamber and on the blinds' surface increased. Conversely, when fully opened, higher temperatures were observed behind the blinds. These results confirm the critical role of shading devices in optimizing thermal efficiency [6]. Another simulation study indicated that the presence of Venetian blinds influences the temperature and air distribution in the DSF system. For the cases considered, the changes in the position of the blinds have higher effect on the distribution of temperature and velocity compared to the changes in the slat angles [11]. Despite these advances, a gap in understanding the impact of blinds positioning on DSF cavity air temperature under different airflow conditions in our climate still remains. The spring season, with its significant temperature variations between day and night and fluctuating solar radiation, provides ideal conditions for studying these effects. The aim of this work is to assess the effect of the position of blinds on the air temperature in the cavity of the double skin facade during the spring period on the building of the University Science Park – Technicom in Kosice. The building has been designed and built with a double-skin transparent facade. There are two types of facades on the building, the first type on the west side of the building and the second type on the south side of the building. The double-skin transparent facade is designed as a corridor that runs at the full height of the building. The south side of the DSF is designed with the ability to control and regulate the air in the cavity. The airflow can be influenced by changing the geometry of the cavity, the intensity of the air flow, the position and the permeability of the shading system and possible combinations of these. The space between the floors is divided by galvanised bars mounted on brackets. These constructions do not prevent airflow over the entire height and width of the space. The cavity space is divided into eight separate units. Adjustable outlets allow these units to be changed to four, two or one unit as required.

The following tasks were set to achieve this objective:

1. Determining the effect of the blinds position on the air temperature in the DSF cavity,
2. Determining the effect of the ventilation height cavity on the air temperature.
3. Comparing two methods of blind positioning over a period of time,
4. Comparing two cavity geometries,
5. Carrying out measurements and processing the measured data,
6. Comparing and evaluating the research results.

2 METHODOLOGY

The measurement was carried out over a period of 35 days during the spring season. Temperature comparisons and analysis of the results were carried out under three climatic conditions: sunny, cloudy and semi-cloudy. In the first part of the measurement, the facade was set in the facade operating mode (FOM) – A (Fig. 1a), which operates on the basis of airflow at a height of one field and a width of two fields. In the second part of the measurement, the facade was set in facade operating mode – D (Fig. 1b). Mode D operates on the basis of airflow at the height of the four fields and across all widths of the facade. On the entire facade, the blinds were set in the front and rear positions. The front blinds were lowered in the CD field and raised in the AB field. The rear blinds were raised in the CD field and lowered in the AB field. Values were also recorded on the west side of the facade to compare the two facade types on the building. The recorded values were filtered after the measurements were completed. The measurement points shown in Tab. 1 were used for comparison. Air temperatures in the cavity were measured in AB and CD fields (Fig. 2). There were 2 radiators off in the room and the radiator under the south elevation was set to IIII. Individual measuring points were connected to the datalogger. Measurements were taken at all sensors of the measuring points. The measurements were recorded automatically via the datalogger. The measurement time step was 1 minute.

Tab. 1 Measuring points used.

Marking of data	Unit	Quantity	Position
TAIR_INT	°C	Interior air temperature	
Tsi_conv1	°C	Radiator temperature	
Tair_EXT	°C	Exterior air temperature	
Glob_rad	$W.m^{-2}$	Global solar radiation	Roof
D_300	°C	Air temperature in the cavity	AB field
D_700	°C	Air temperature in the cavity	CD field
FW	°C	Air temperature in the cavity	West side

DOI 10.13164/juniorstav.2025.26102

Solar radiation was recorded using the FLA628S pyranometer to measure global, solar and shortwave reflectance. The spectral range was 0.3 - 3 micrometres. The measuring range was 0 - 150 $W.m^{-2}$. The outside temperature was measured by a weather station with an NTC sensor with a resolution of 0.1 K and an accuracy of + 0.2 K. The cavity temperature sensors were NiCr-Ni thermocouples with an accuracy of ± 0.004 x | t | K.

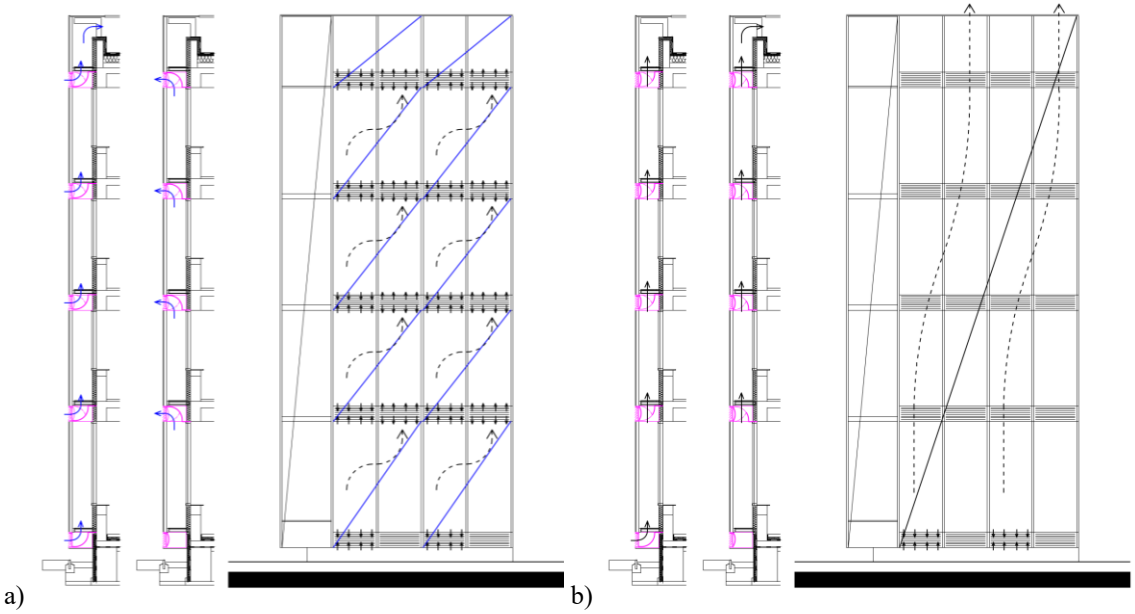

Fig. 1 Facade operating mode A a) and D b).

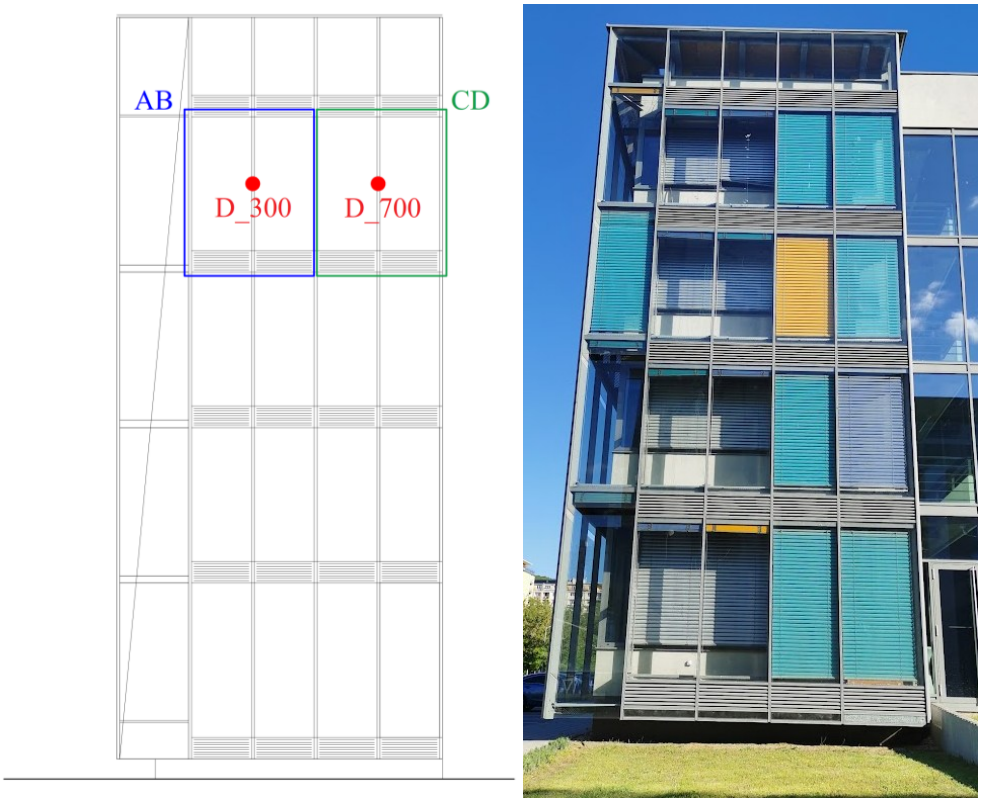

Fig. 2 Sensor positions as seen from the exterior façade.

DOI 10.13164/juniorstav.2025.26102

3 RESULTS

Sunny day

Cavity air temperatures increased constantly with the intensity of global solar irradiance. The temperature on the west facade did not grow as fast as on the south facade. It did not reach values similar to the experimental part of the facade in either operating mode throughout the day. The results are presented in diagrams (Fig. 3, Fig. 4).

Facade operating mode A:

The diagram in Fig. 3 shows cavity temperatures on a sunny day in FOM A. The temperature in field AB reached a maximum value of 32.1°C at 10:33, and in field CD 26.8°C at 12:14. The temperatures in the operating mode of facade A reached higher values at position D_300 than at D_700. The temperature in the AB field had both a faster rise and higher values than in the CD field. The outdoor air temperature ranged from 2.1°C to 14.1°C. The indoor air temperature ranged from 21.1°C to 22.4°C. The maximum temperature at the radiator was 36.1°C at 5.28 a.m. The minimum temperature was at 4:31 p.m. when it reached 22.5 °C, which was close to the indoor temperature. The temperature on the radiator started to rise during the morning hours when it was necessary to reach the desired indoor temperature. As the sun rose and the cavity gradually warmed, the temperature of the radiator began to fall. Due to the higher temperature in the cavity, it was not necessary to heat the radiator evenly throughout the day.

Facade operating mode D:

The diagram in Fig. 4 shows cavity temperatures on a sunny day in FOM D. The temperature in the AB field reached a maximum value of 20.7°C at 11:28 a.m. and in the CD field 19.5°C at 11:27 a.m. The temperatures in the operating mode of facade D at position D_300 were relatively similar to those at D_700. The temperature at the sensor in the AB field also had a similar increase and similar values to the CD field. The outdoor air temperature ranged from -1.09°C to 9.54°C. The indoor air temperature ranged from 21.5°C to 22.4°C. The maximum temperature at the radiator was in the early morning hours when it reached 34.2 °C at 04:25, and the minimum temperature was 23.00°C at 5:31 p.m. The temperature at the radiator started to rise in the morning hours. In this FOM the temperature decreased more slowly and did not reach such constant values as in FOM A. As the cavity temperature decreased, the internal temperature decreased and the radiator temperature had to be increased. The drop in the cavity temperature is related to the air circulation, which leads to faster cooling.

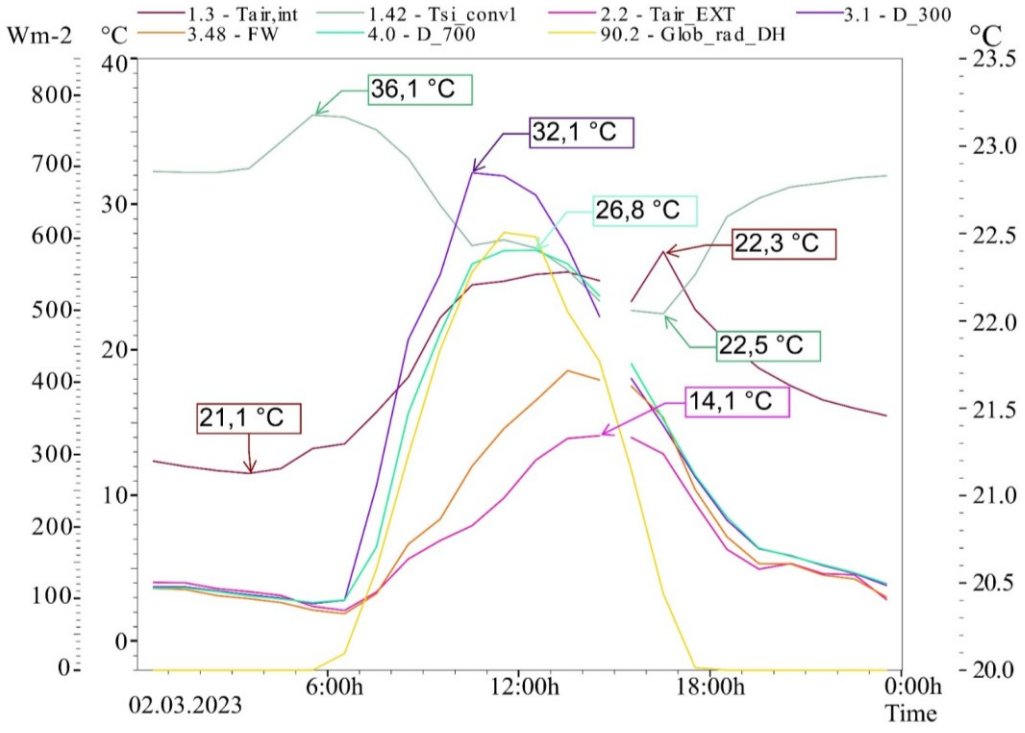

Fig. 3 DSF cavity temperatures on a sunny day in FOM A.

DOI 10.13164/juniorstav.2025.26102

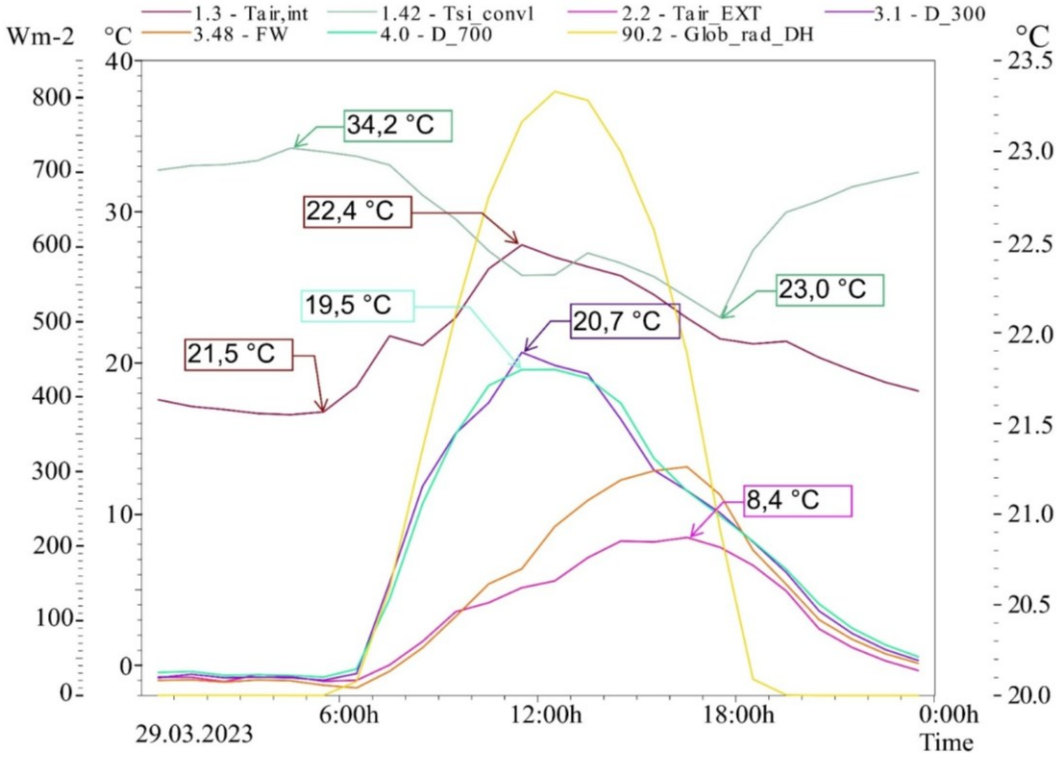

Fig. 4 DSF cavity temperatures on a sunny day in FOM D.

Cloudy day

On a cloudy day, the global solar radiation intensity was very low. Due to this factor, the cavity air temperatures increased more slowly. The temperature on the west facade did not rise as quickly as on the south facade. It did not reach values similar to the experimental part of the facade throughout the day. The temperature was approximately the same as the outdoor air temperature.

Facade operating mode A:

The diagram in Fig. 5 shows cavity temperatures on a sunny day in FOM A. The temperature in the AB field reached a maximum of 9.2°C at 10:31, and in the CD field 8.6°C, also at 1:35 p.m.. The temperatures at all sensor positions increased at the same rate. The temperature at position D_300 in field AB increased faster, but decreased during the day and increased with the intensity of solar radiation. The temperature at sensor D_700 in array CD had a smoother curve. The outdoor air temperature ranged from -0.1°C to 5.3°C. The indoor air temperature ranged from 21.3°C to 21.7°C. The minimum radiator temperature was 29.8°C at 11:31, and the maximum was 34.8°C at 8:30. The radiator temperature was stable until the morning hours when it increased with the indoor temperature. The radiator temperature decreased during the midday hours when solar radiation reached higher values.

Facade operating mode D:

Fig. 6 DSF cavity temperatures on a cloudy day in FOM D.

shows chart of cavity temperatures on a sunny day in FOM D. The temperature in the AB field reached a maximum value of 9.4°C at 10:59, in the CD field 9.8°C at 11:11. The temperatures at all sensor positions increased at the same rate. In this case, the temperature at position D_700 in the CD array had higher values than at position D_300 in the AB array. The outdoor air temperature ranged from 2.6°C to 8.3°C. The indoor air temperature ranged from 21.7°C to 22.2°C. The minimum radiator temperature was 26.5°C at 02:33 and the maximum was 31.6°C at 22:45. The radiator temperature was constant throughout the day due to low solar radiation and low cavity temperatures. The temperature on the radiator began to rise in the afternoon as the cavity cooled and the outdoor temperature dropped.

DOI 10.13164/juniorstav.2025.26102

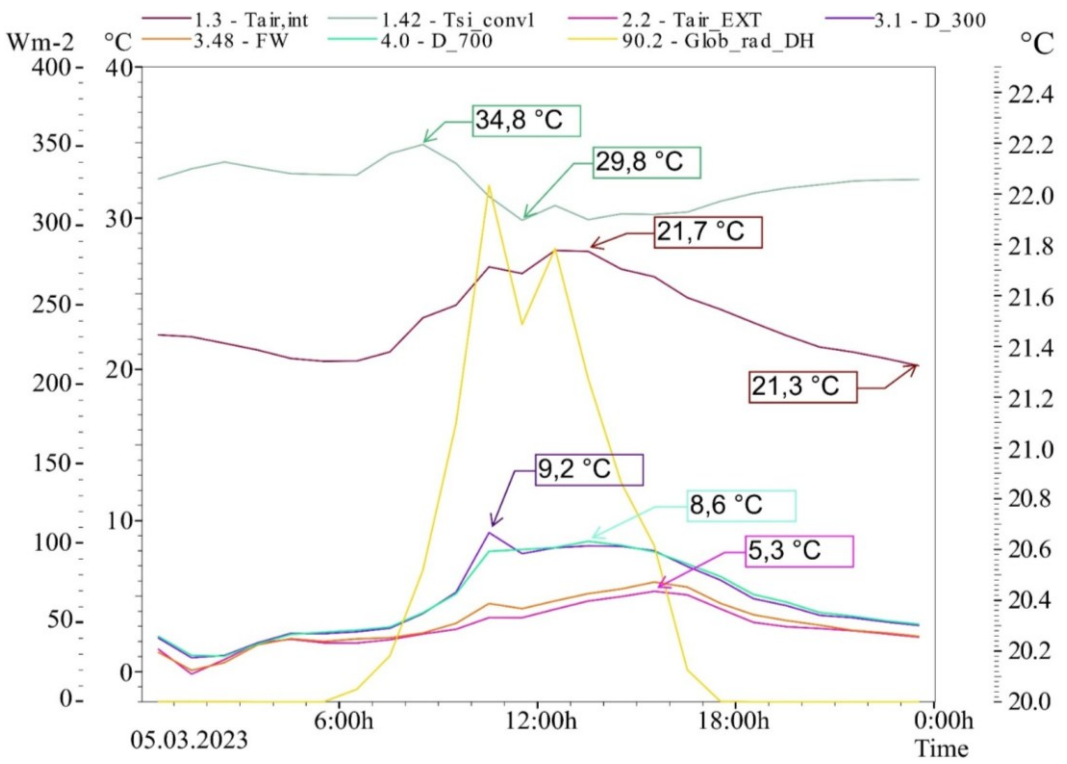

Fig. 5 DSF cavity temperatures on a cloudy day in FOM A.

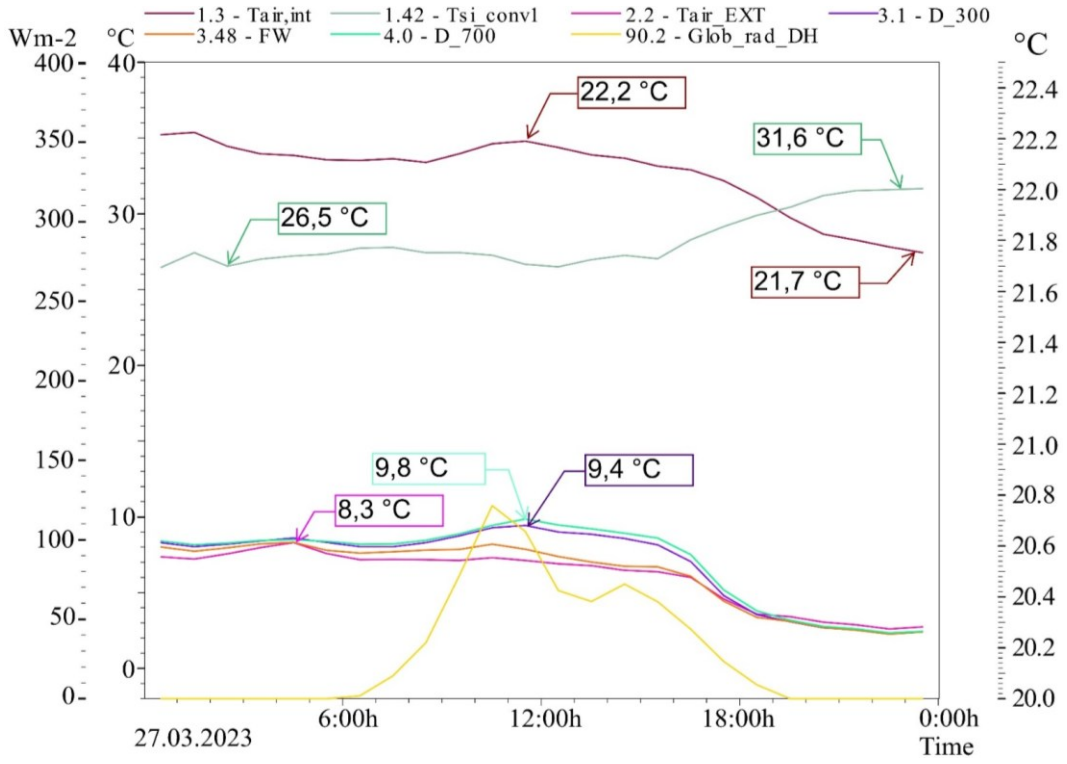

Fig. 6 DSF cavity temperatures on a cloudy day in FOM D.

DOI 10.13164/juniorstav.2025.26102

4 DISCUSSION

Values from three climatic boundary conditions were used for comparison. Data from 5 March 2023 were used as a cloudy day for the operation mode of facade A (Fig. 7), 2 March 2023 as a sunny day and 6 March 2023 as a partly cloudy day. Data from 27 March 2023 was used as a cloudy day, 29 March 2023 as a sunny day and 11 March 2023 as a partly cloudy day for the operation mode of facade D (Fig. 8). It can be confirmed from this comparison that the temperature of the cavity air is dependent on the intensity of the global solar radiation and the temperature outside. The cavity temperature on the west facade did not reach the same values as the sensors on the south side. The highest temperatures were reached at times when the south facade was cooling down. The measurements confirmed the correct way of cooling the cavity during the night hours. The air temperature in the cavity affects the heating system. The temperature of the radiator drops faster at higher cavity temperatures, it does not heat.

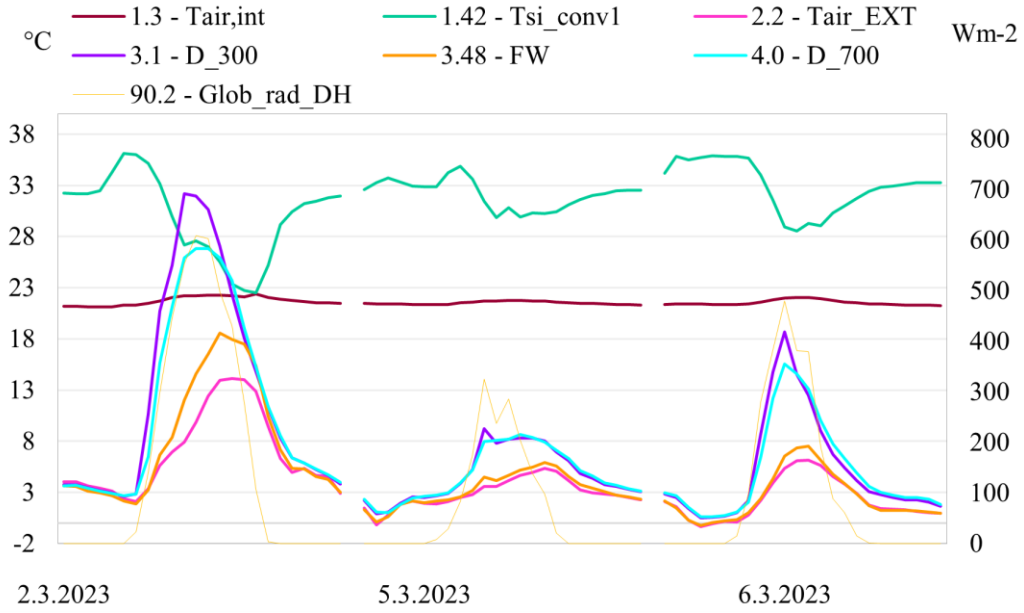

Fig. 7 DSF cavity temperatures on a sunny day in FOM A.

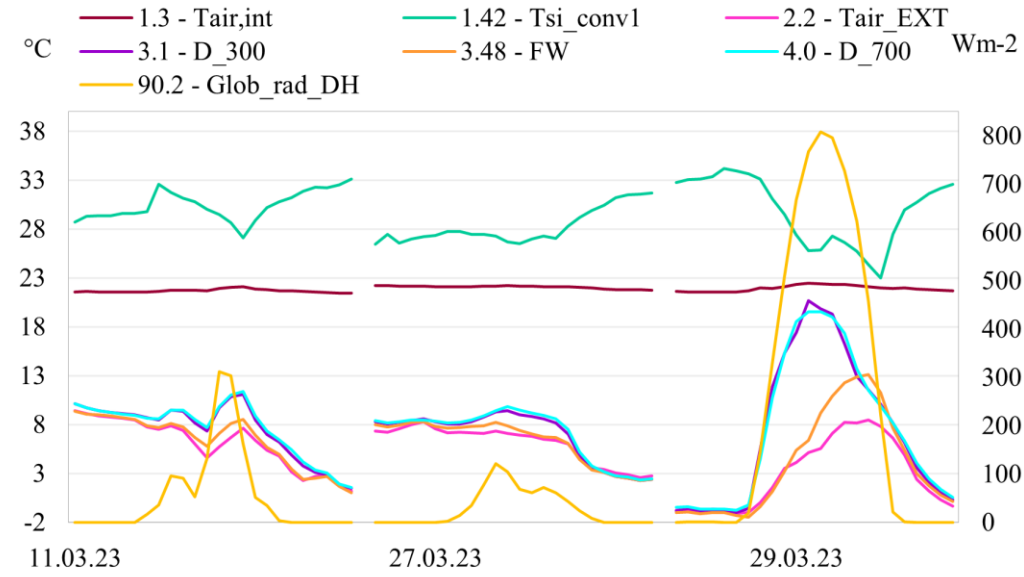

Fig. 8 DSF cavity temperatures on a sunny day in FOM D.

DOI 10.13164/juniorstav.2025.26102

Comparison of operating modes

The temperature differences in FOM A between sensors D ranged from 0 K to 7 K on a sunny day (Fig. 9a). The temperature differences were lower but still reached values of 0 K to 6 K on a partly cloudy day. These differences were the lowest on a cloudy day, with the difference ranging up to 2 K. The temperature differences in FOM D between sensors D reached values up to 2 K on a sunny day (Fig. 9b). The temperature differences were lower but still reached values up to 1 K on a partly cloudy day. These differences were naturally the lowest on a cloudy day, with the difference reaching up to 1 K. The temperatures during a cloudy to partly cloudy day did not show so large differences between them as for FOM A.

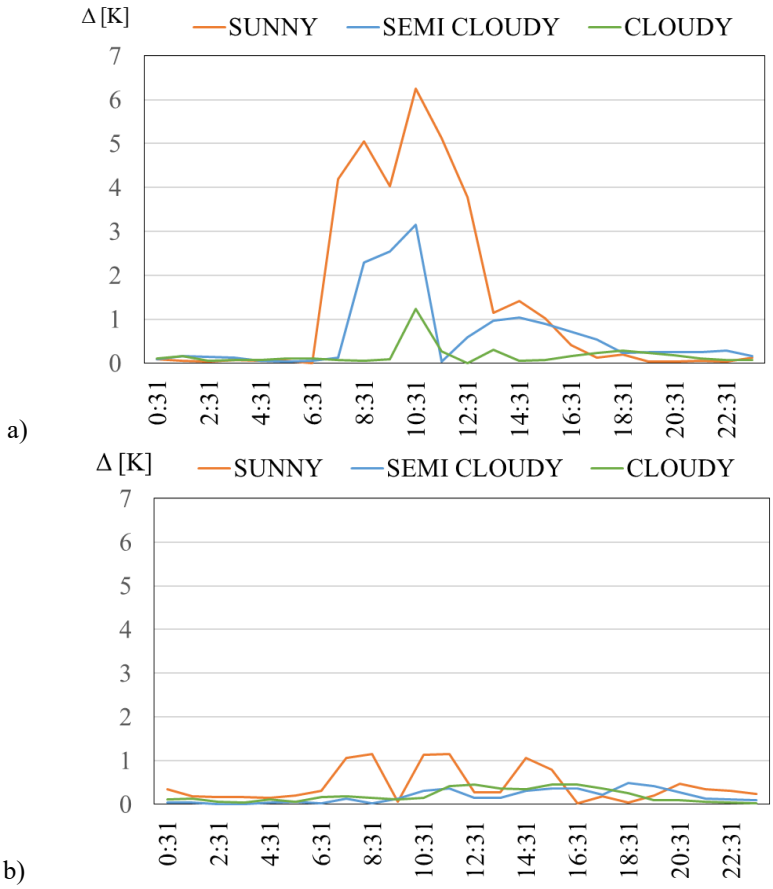

Fig. 9 Temperature difference at sensor position D in FOM A a) and D b) during boundary conditions.

The temperature differences of the air in the cavity during a sunny day ranged from 0 K to 7 K (Fig. 10a). Comparing the two operating modes, the cavity air temperatures were higher for FOM A. It can be concluded that the cavity air temperature was higher due to the smaller airflow circuit. In FOM D the cavity air temperature was lower due to the larger air circuit. The cavity air temperature differences during a cloudy day ranged from 0 K to 2 K (Fig. 10b). The cavity air temperatures were higher for FOM A.

DOI 10.13164/juniorstav.2025.26102

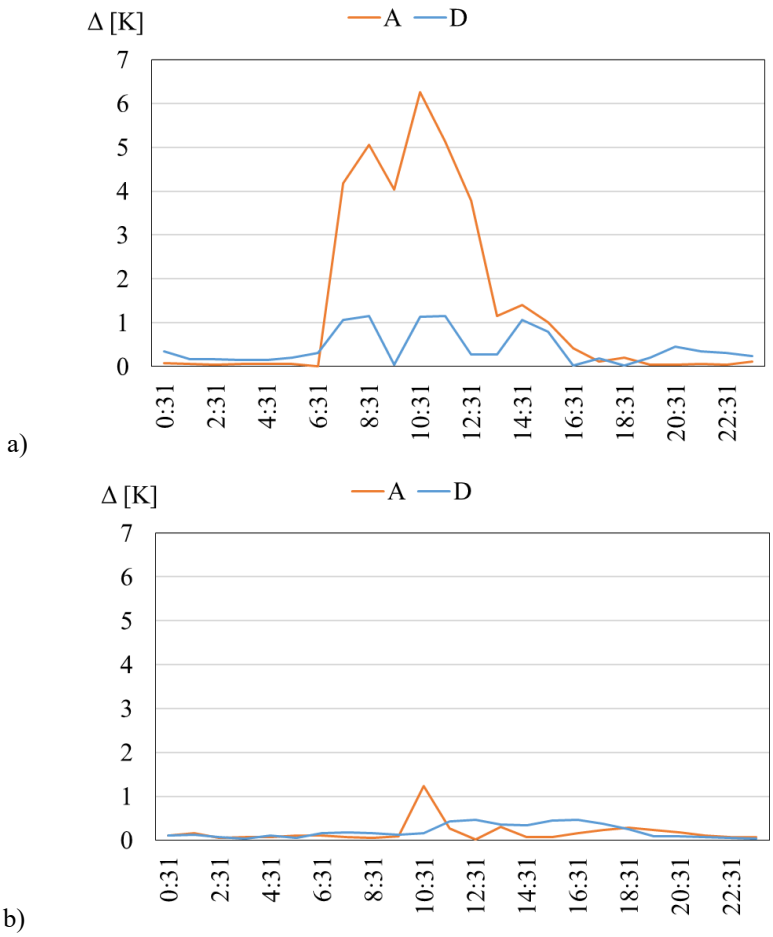

Fig. 10 Temperature difference at sensor position D in FOM A and D on a sunny a) and cloudy b) day.

The comparison shows that there is a difference between the blinds being raised and lowered in both operating modes. On a sunny day, higher interstitial air temperatures were reached in the AB field which had the front blinds drawn and the rear blinds lowered.

5 CONCLUSION

The position of the blinds affects the air temperature in the cavity of the double skin-facade. It was assumed that higher temperatures would be reached in the field with the front blinds closed. It was confirmed that during the climatic boundary conditions in spring, the air temperatures in the cavity reached higher values in the field where the front blinds were down. The differences ranged from 0 to 7 K in FOM A and from 0 to 2 K in FOM D. Lower air temperatures were in the CD field with the blinds closed. The temperature differences at sensor D were higher than facade operating mode D during facade operating mode A. Comparing the two façade operating modes, it can be concluded that the smaller airflow circuit results in larger temperature differences between the AB and CD fields. Cavity air temperature also influences the number of heating hours in a given operating mode. It can be concluded that it is preferable to use mode A during the colder seasons with the rear blinds down. This is due to the use of a small airflow circuit when higher temperatures occur in the cavity. It is preferable to use mode D during periods when the heating demand is lower due to the airflow over the entire height of the facade. In this case, it is preferable to use the front blinds down. In this mode, the temperatures in the cavity are not as high as when the facade is closed at a lower height. The temperatures in the cavity on the west facade did not reach as high values as on the south facade throughout the measurement. Further measurements are needed to address the issue of how the facade performs in other climatic conditions. It is also possible to investigate these parameters in other operating modes of the facade with the different adjustment possibilities. The aim of further measurements

DOI 10.13164/juniorstav.2025.26102

will be to determine the appropriate interface of operation modes to be used for the heating and cooling needs of the building. It is necessary to determine when the interstitial air temperature indicates losses and gains.

Acknowledgements

This paper was elaborated with the financial support of the research project VEGA 1/0499/23 of the Scientific Grant Agency of the Ministry of Education, Research, Development and Youth of the Slovak Republic and the Slovak Academy of Sciences.

References

[1] WEN, Yuangao, Qiongqiong GUO, Pin An XIAO and Tingzhen MING. The Impact of Opening Sizing on the Airflow Distribution of Double-skin Facade. In: Procedia Engineering [online]. 2017. ISSN 18777058.
[2] HOU, Keming, Shanshan LI and Haining WANG. Simulation and experimental verification of energy saving effect of passive preheating natural ventilation double skin facade. Energy Exploration and Exploitation [online]. 2021, 39(1). ISSN 20484054.
[3] PELLETIER, Kate, Christopher WOOD, John CALAUTIT and Yupeng WU. The viability of double-skin facade systems in the 21st century: A systematic review and meta-analysis of the nexus of factors affecting ventilation and thermal performance, and building integration [online]. 2023. ISSN 03601323.
[4] AHMED, Mostafa M. S., Ali K. ABEL-RAHMAN, Ahmed Hamza H. ALI and M. SUZUKI. Double Skin Facade: The State of Art on Building Energy Efficiency. Journal of Clean Energy Technologies [online]. 2015, 4(1). ISSN 1793821X.
[5] BARBOSA, Sabrina and Kenneth IP. Perspectives of double skin facades for naturally ventilated buildings: A review [online]. 2014. ISSN 13640321.
[6] PARRA, Jordi, Alfredo GUARDO, Eduard EGUSQUIZA and Pere ALAVEDRA. Thermal performance of ventilated double skin facades with venetian blinds. Energies [online]. 2015, 8(6). ISSN 19961073.
[7] POIRAZIS, Harris. Double-skin facades – A literature review. IEA SHC Task 34. 2007, 49(10). ISSN 00012491.
[8] HONG, Xiaoqiang, Junwei LIN, Xuan YANG, Shaosen WANG and Feng SHI. Comparative Analysis of the Daylight and Building-Energy Performance of a Double-Skin Facade System with Multisectional Shading Devices of Different Control Strategies. Journal of Energy Engineering [online]. 2022, 148(3). ISSN 0733-9402.
[9] YONG, Seok Gil, Jong Hyun KIM, Yuseong GIM, Jinho KIM, Jinkyun CHO, Hiki HONG, Young Jin BAIK and Junemo KOO. Impacts of building envelope design factors upon energy loads and their optimization in US standard climate zones using experimental design. Energy and Buildings [online]. 2017, 141. ISSN 03787788.
[10] MOAZZENI KHORASGANI, Ali, NILOOFAR ZAREARSANJANI and ARLYN RODRIGUEZ. Using IoT in Double Skin Facades toward Thermal Comfort: A Review. Urban Planning and Construction [online]. 2023, 2(1).
[11] JIRU, Teshome Edae, Yong X. TAOB and Fariborz HAGHIGHAT. Airflow and heat transfer in double skin facades. Energy and Buildings [online]. 2011, 43(10). ISSN 03787788.